ESD-TR-68-275

WP-2015

BACKGROUND FOR NARROWBAND INTERFEROMETRY

I. ISOTROPIC POINT SCATTERERS

H. S. Ostrowsky

NOVEMBER 1968

Prepared for

SPACE DEFENSE AND COMMAND SYSTEMS PROGRAM OFFICE
ELECTRONIC SYSTEMS DIVISION
AIR FORCE SYSTEMS COMMAND
UNITED STATES AIR FORCE
L. G. Hanscom Field, Bedford, Massachusetts

Project 4966
Prepared by
THE MITRE CORPORATION
Bedford, Massachusetts
Contract AF19(628)-5165

ESD-TR-68-275 WP-2015

BACKGROUND FOR NARROWBAND INTERFEROMETRY
I. ISOTROPIC POINT SCATTERERS

H. S. Ostrowsky

NOVEMBER 1968

Prepared for

SPACE DEFENSE AND COMMAND SYSTEMS PROGRAM OFFICE
ELECTRONIC SYSTEMS DIVISION
AIR FORCE SYSTEMS COMMAND
UNITED STATES AIR FORCE
L. G. Hanscom Field, Bedford, Massachusetts

Project 4966
Prepared by
THE MITRE CORPORATION
Bedford, Massachusetts
Contract AF19(628)-5165

FOREWORD

This technical report has been prepared by The MITRE Corporation, Department D-85, under Contract AF19(628)-5165, Project 4966. The contract is sponsored by the Electronic Systems Division, Air Force Systems Command, L. G. Hanscom Field, Mass.

REVIEW AND APPROVAL

This technical report has been reviewed and is approved.

HENRY J. MAZUR, Colonel, USAF
Director, Space Defense & Command Systems Pgm Ofc
Deputy for Surveillance & Control Systems

ABSTRACT

A recent paper described a method for using narrowband interferometry at small bistatic angles to obtain two and three dimensional images of targets in terms of their scattering centers. The present paper is intended primarily to provide additional background information and a theoretical foundation for such narrowband interferometry and to consider some of its limitations, and secondly to indicate what information is to be found in the data and how it might be used.

TABLE OF CONTENTS

SECTION I

INTRODUCTION

A recent paper[1] described a method for using narrowband interferometry at small bistatic angles to obtain two and three dimensional images of targets in terms of their scattering centers. The present paper is intended primarily to provide additional background information and a theoretical foundation for such narrowband interferometry and to consider some of its limitations, and secondly to indicate what information is to be found in the data and how it might be used. This latter presentation will be brief, since I intend to provide a more thorough discussion concerning data processing schemes in a later paper.

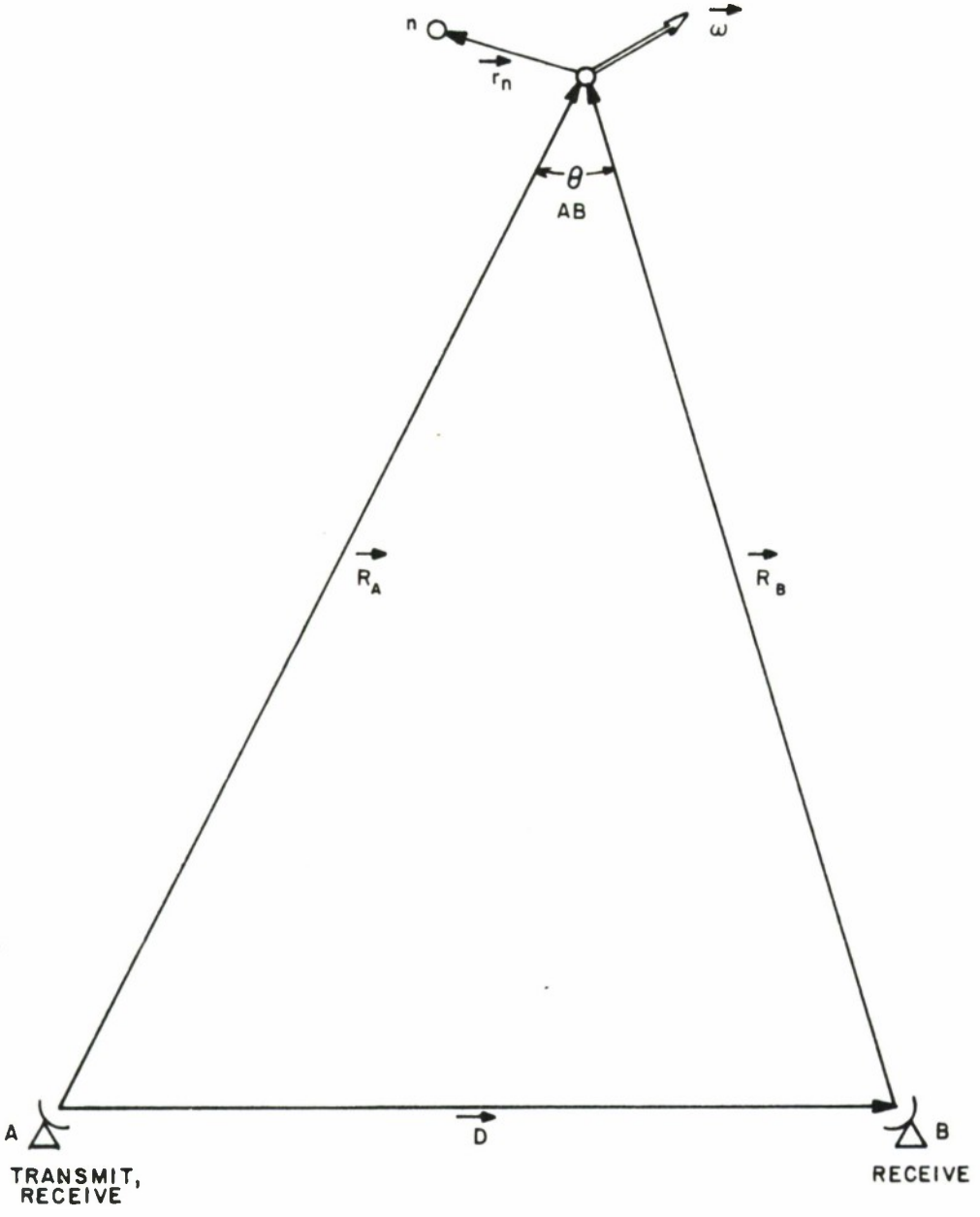

Figure 1. Geometry for a Two-Site Interferometer (Not to Scale)

SECTION II

THE FORM OF THE RECEIVED SIGNAL

In this section we will consider a target composed of N point scatterers rigidly connected to a center of gravity 0 (by means of the usual invisible rods) and rigidly rotating about 0 with constant angular velocity $\vec{\omega}$, whilst at the same time 0 is being translated with velocity $\vec{V}(t)$. This target is being tracked continuously by a radar interferometer consisting of a narrowband transmitter-receiver located on the ground at A, and remote receivers located at B and C, each capable of measuring phase. The angle subtended by the interferometer system at the target is assumed to be small. Referring to Figure 1, the location of each scatterer relative to 0 is given by vector $\vec{r}_n$. Electromagnetic radiation striking each scatterer is assumed to be reradiated isotropically, and each scatterer is characterized by a complex number $H_n e^{j\Psi_n}$, where H_n gives the relative strength of the re-radiated signal and Ψ_n gives the phase change upon re-radiation; for the present these numbers are assumed to be constants for each scatterer. The velocity of scatterer n is given by

$$\vec{V}_n = \vec{V} + \vec{\omega} \times \vec{r}_n \quad . \tag{1}$$

The vector from radar A to target center 0 is called $\vec{R}_A$, and similarly for B and C.

The target is assumed to be small in the sense that $\min\{R\} \gg \max\{r_n\}$ and $\max\{\hat{R} \cdot \vec{r}_n\} \ll \frac{c\Delta}{2}$ where Δ is the length of the transmitted pulse in seconds. This condition is trivially satisfied for all reasonable targets, distances, and narrowband pulse length. The radars operate

at frequency f_o, where for concreteness in visualization we may consider radar parameters like those of the present MITRE-Lincoln Lab interferometer, i.e., $f_o \simeq 10^3$ MHz and $\Delta \simeq 1$ ms.

Under the above assumptions the wave which strikes each scatterer can be well approximated by a plane wave whose frequency appears (to the scatterer n) to be

$$f_n^A \simeq f_o(1 - \frac{1}{c}\vec{v}_n \cdot \hat{R}_A) = f_o(1 - \frac{1}{c}\vec{V} \cdot \hat{R}_A) + \frac{f_o}{c}\hat{R}_A \times \vec{r}_n \cdot \vec{\omega} , \tag{2}$$

due to the doppler shift. Taking the x-direction along $\hat{R}_A$ we can write the incoming wave near scatterer n as

$$I_n \sim e^{j\phi_o} \exp[2\pi j \frac{f_n^A}{c}(x - ct)] . \tag{3}$$

Notice that the wave reaches each scatterer n, at location $x_n \equiv R_A + \hat{R}_A \cdot \vec{r}_n$, at time $t_n \equiv x_n/c$, so that $I_n \sim e^{j\phi_o}$ at each scatterer as the wave front of the pulse strikes it. For re-radiation, two cases must now be considered.

Case I RE-RADIATION BACK IN THE DIRECTION OF TRANSMITTER A.

The wave re-radiated by scatterer n goes in the direction $-\hat{R}_A$. The doppler shift causes an additional change of frequency, such that the new frequency is

$$f_n^{AA} = f_n^A(1 - \frac{1}{c}\vec{v}_n \cdot \hat{R}_A) \simeq f_o(1 - \frac{2}{c}\vec{V} \cdot \hat{R}_A) + 2\frac{f_o}{c}\hat{R}_A \times \vec{r}_n \cdot \vec{\omega} . \tag{4}$$

As it approaches the receiver A the signal again looks like a plane wave, and can be written in the from

$$S_n^A \sim H_n e^{j(\phi_o + \Psi_n)} \exp\{2\pi j \frac{f_n^{AA}}{c} [(x - x_n) + c(t - t_n)]\} . \qquad (5)$$

The nominal time of arrival of the re-radiated wave front of the pulse at the receiver A (at $x \equiv 0$) is $t = 2R_A/c$, giving the time from the object's center 0. Substituting $x = 0$ and $t = 2R_A/c$ into Equation (5), gives the form of the received wave front from scatterer n as

$$S_n^A \sim H_n e^{j(\phi_o + \Psi_n)} \exp[-4\pi j \frac{f_n^{AA}}{c} (\hat{R}_A \cdot \vec{r}_n)] .$$

Adding the results from all the scatterers, making use of Equation (4), and recalling that $\lambda_o \equiv c/f_o$, we get for the total received signal at A:

$$S^A \sim e^{j\phi_o} \sum_{n=1}^{N} H_n e^{j\Psi_n} \exp[-\frac{4\pi}{\lambda_o} j(1 - \frac{2}{c} \vec{V} \cdot \hat{R}_A + \frac{2}{c} \hat{R}_A \times \vec{r}_n \cdot \vec{\omega}) (\hat{R}_A \cdot \vec{r}_n)] . \qquad (6)$$

But for reasonable objects $r_n < 10$ m., $\omega < 1$ rad/sec, and $V \lesssim 10^4$ m/sec, whereupon $|\frac{2}{c} \vec{V} \cdot \hat{R}_A| < 10^{-4}$ and $|\frac{2}{c} \hat{R}_A \times \vec{r}_n \cdot \vec{\omega}| < 10^{-7}$. Accordingly we can ignore the second and third terms in the parenthesis in comparison with the first term, leaving

$$S^A \sim e^{j\phi_o} \sum_{n=1}^{N} H_n e^{j\Psi_n} \exp(-4\pi j \frac{r_n}{\lambda_o} \hat{R}_A \cdot \hat{r}_n) . \qquad (7)$$

Case II RE-RADIATION IN THE DIRECTION OF REMOTE RECEIVER B.

The wave re-radiated by scatterer n goes in the direction $-\hat{R}_B$. The doppler shift causes an additional change of frequency, such that the new frequency is

$$f_n^{AB} \simeq f_n^A \left(1 - \frac{1}{c} \vec{v}_n \cdot \hat{R}_B\right) \simeq f_o \left[1 - \frac{1}{c} \vec{v}_n \cdot (\hat{R}_A + \hat{R}_B)\right] . \quad (8)$$

Now if we define

$$\hat{R}_{AB} \equiv \frac{\hat{R}_A + \hat{R}_B}{|\hat{R}_A + \hat{R}_B|} \quad (9a)$$

and

$$\cos\theta_{AB} \equiv \hat{R}_A \cdot \hat{R}_B , \quad (9b)$$

then it is easily seen that

$$\hat{R}_A + \hat{R}_B \equiv 2\hat{R}_{AB} \cos\left(\frac{\theta_{AB}}{2}\right) , \quad (10)$$

whereupon Equation (8) becomes

$$f_n^{AB} \simeq f_o \left[1 - \frac{2}{c} \vec{v}_n \cdot \hat{R}_{AB} \cos\left(\frac{\theta}{2}\right)\right] \simeq f_o \left[1 - \frac{2}{c} \vec{V} \cdot \hat{R}_{AB} \cos\left(\frac{\theta}{2}\right)\right]$$

$$+ 2\frac{f_o}{c} \hat{R}_{AB} \times \vec{r}_n \cdot \vec{\omega} \cos\left(\frac{\theta}{2}\right) . \quad (11)$$

As it approaches the receiver B the signal again looks like a plane wave, and can be written in the form

$$S_n^B \approx H_n e^{j(\phi_o + \Psi_n)} \exp\{2\pi j \frac{f_n^{AB}}{c} [(y - y_n) + c(t - t_n)]\} , \quad (12)$$

where the y-direction is taken along $\hat{R}_B$, $y_n \equiv R_B + \hat{R}_B \cdot \vec{r}_n$, and t_n as before. The nominal time of arrival of the re-radiated wave front of the pulse at the receiver B (at $y \equiv 0$) is $t = (R_A + R_B)/c$, giving the time from the object's center 0 . Substituting into Equation (12) gives the form of the received wavefront from scatterer n as

$$S_n^B \sim H_n e^{j(\phi_o + \Psi_n)} \exp [-4\pi j \frac{f_n^{AB}}{c} \hat{R}_{AB} \cdot \vec{r}_n \cos (\frac{\theta}{2})] .$$

By adding the terms due to each scatterer and proceeding as in Case I we finally get the total received signal at B:

$$S^B \sim e^{j\phi_o} \sum_{n=1}^{N} H_n e^{j\Psi_n} \exp \left[-4\pi j \frac{r_n}{\lambda_o} \hat{R}_{AB} \cdot \hat{r}_n \cos\left(\frac{\theta_{AB}}{2}\right)\right] . \quad (13)$$

A similar analysis can of course be done for remote receiver C also; the result is Equation (13) with B everywhere replaced by C .

SECTION III

TIME DEPENDENCE OF THE RECEIVED SIGNAL

The values for the received signal S given by Equations (7) and (13) are for one pulse only. To find out how S varies from pulse to pulse we must find an expression for the time dependence of S. The assumption of isotropic re-radiation which we have made implies that the time dependence cannot involve H_n or Ψ_n. Therefore the only quantities which can contain the time dependence are $\hat{R}_A \cdot \hat{r}_n$ in Equation (7) and $\hat{R}_{AB} \cdot \hat{r}_n \cos\left(\frac{\theta_{AB}}{2}\right)$ in Equation (13). Let us examine these quantities.

We will eventually need to take the finite Fourier Transform of $S(t)$, integrating over a time interval of length T centered on some time t_o: $t_o - \frac{T}{2} \leq t \leq t_o + \frac{T}{2}$. Usually T will be "small," the precise meaning of which will become clear as we proceed. Therefore we will expand all time-dependent functions in Taylor series about t_o and keep only first-order terms in small quantities. *

For $\hat{r}_n(t)$ we note that $\frac{d\hat{r}_n}{dt} = \vec{\omega}(t) \times \hat{r}_n(t)$, whereupon the Taylor Series gives

$$\hat{r}_n(t) \simeq \hat{r}_n(t_o) + (t - t_o)\, \vec{\omega}(t_o) \times \hat{r}_n(t_o) + O\left(\omega \frac{T}{2}\right)^2 . \qquad (14)$$

In order for this linearization to be valid, it is necessary that $\left(\omega \frac{T}{2}\right)^2 \ll 1$ hold true. To be concrete, suppose we require that $\omega T/2 < 0.1$. Then writing $\omega \equiv 2\pi / \tau$, where τ is the period of the object's rotation, this

---

* For certain purposes it may be useful to retain the second-order terms also, but this will not be considered in the present paper.

condition becomes approximately

$$T \lesssim 0.03\ \tau\ . \tag{15}$$

This may be regarded physically as a limitation on the length of the integration interval T in comparison with the body rotation period τ, such that the Fourier Transform not be "smeared-out" by rotation through too large an aspect angle during the integration. If amplitude weighting is used during integration to reduce the contributions of data points near the ends of the interval ($|t-t_o| \sim \frac{T}{2}$) in comparison with data points near the center, then presumably this condition may be relaxed a bit. How much, depends on the form of weighting used; perhaps $T \leq 0.05\ \tau$ would be all right.

The function $\hat{R}_A(t)$ varies quite slowly under most conditions; if we write

$$\frac{d}{dt}\ \hat{R}_A \equiv \vec{\omega}_A(t) \times \hat{R}_A(t)\ , \tag{16}$$

then $\omega_A \lesssim 10^{-2}$ rad/sec except near zero-Doppler of very close asses. Furthermore, $\vec{\omega}_A$ itself changes quite slowly, so that it is reasonable to assume that $\frac{d}{dt}\ \vec{\omega}_A \approx 0$ for $t_o - \frac{T}{2} \leq t \leq t_o + \frac{T}{2}$ even if T is not absolutely small. Therefore we can approximate $\hat{R}_A(t)$ by the first two terms of its Taylor Series expansion:

$$\hat{R}_A(t) \simeq \hat{R}_A(t_o) + (t-t_o)\,\vec{\omega}_A(t_o) \times \hat{R}_A(t_o) + O\left(\omega_A \frac{T}{2}\right)^2 \tag{17}$$

For the bistatic case, if we write

$$\frac{d}{dt}\left[\hat{R}_{AB}\cos\left(\frac{\theta_{AB}}{2}\right)\right] \equiv \vec{\omega}_{AB}(t) \times \hat{R}_{AB}(t)$$

and make use of Equation (10) to express $\hat{R}_{AB}\cos\left(\frac{\theta_{AB}}{2}\right)$ in terms of $\hat{R}_A$ and $\hat{R}_B$, then it turns out that the difference between $\vec{\omega}_{AB}$ and $\vec{\omega}_A$ is of second order in small quantities. Therefore we can write, analogously to Equation (17),

$$\hat{R}_{AB}(t) \simeq \hat{R}_{AB}(t_o) + (t-t_o)\,\vec{\omega}_A(t_o) \times \hat{R}_{AB}(t_o) + O\left(\omega_A \frac{T}{2}\right)^2 . \tag{18}$$

Notice that, if desired, the geometrical constraints would allow us to express $\hat{R}_{AB}(t)$ in terms of $\hat{R}_A(t)$, $\vec{\omega}_A(t)$, and $\vec{D}$.

Now, combining Equations (14), (17), and (7) leads to the expression

$$S^A(t) \sim e^{j\phi_o} \sum H_n e^{j\Psi_n} \exp\left\{-4\pi j \frac{r_n}{\lambda_o}\left[\hat{R}_A(t_o)\cdot\hat{r}_n(t_o) - (t-t_o)\,\hat{R}_A(t_o)\times\hat{r}_n(t_o)\cdot\vec{\Omega}(t_o)\right]\right\}, \tag{19}$$

where

$$\vec{\Omega}(t) \equiv \vec{\omega}(t) - \vec{\omega}_A(t) \tag{20}$$

Similarly, from Equations (14), (18), and (13),

$$S^B(t) \sim e^{j\phi_o} \sum_{n=1}^{N} H_n e^{j\Psi_n} \exp\{-4\pi j \frac{r_n}{\lambda_o} \cos(\frac{\theta}{2}) [\hat{R}_{AB}(t_o) \cdot \hat{r}_n(t_o)$$

$$- (t-t_o)\hat{R}_{AB}(t_o) \times \hat{r}_n(t_o) \cdot \vec{\Omega}(t_o)]\}, \quad (21)$$

with

$$\vec{\Omega}(t) \simeq \vec{\omega}(t) - \vec{\omega}_A(t) \quad (22)$$

as before.

These return signals are compared with the reference signal for phase; this eliminates the phase factor ϕ_o but adds a "range phase" term. We assume that this range phase can be removed by an appropriate phase extraction process, and we assume this has been done. The resulting signals are ready to be integrated in the Fourier Transform.

SECTION IV

TAKING THE FOURIER TRANSFORM

The finite Fourier Transform is defined by

$$\tilde{S}(f) \equiv \int_{t_o - \frac{T}{2}}^{t_o + \frac{T}{2}} S(t)\, e^{-2\pi j f(t-t_o)}\, dt \,. \tag{23}$$

Operating thus on Equation (19) leads to

$$\tilde{S}^A(f) \sim T \sum_{n=1}^{N} H_n e^{j\Psi_n} \exp\left[-4\pi j \frac{r_n}{\lambda_o} \hat{R}_A(t_o) \cdot \hat{r}_n(t_o)\right] \operatorname{sinc}\left[T(f-f_n^A)\right], \tag{24}$$

where

$$\operatorname{sinc}\ \xi \equiv \frac{\sin \pi\ \xi}{\pi\ \xi} \tag{25}$$

and

$$f_n^A \equiv \frac{2r_n}{\lambda_o} \hat{R}_A(t_o) \times \hat{r}_n(t_o) \cdot \vec{\Omega}(t_o) \,. \tag{26}$$

Similarly, from Equation (21),

$$\tilde{S}^B(f) \sim T \sum_{n=1}^{N} H_n e^{j\Psi_n} \exp\left[-4\pi j \frac{r_n}{\lambda_o} \hat{R}_{AB}(t_o) \cdot \hat{r}_n(t_o) \cos\left(\frac{\theta}{2}\right)\right] \operatorname{sinc}\left[T(f-f_n^B)\right] \tag{27}$$

where

$$f_n^B \equiv \frac{2r_n}{\lambda_o} \hat{R}_{AB}(t_o) \times \hat{r}_n(t_o) \cdot \vec{\Omega}(t_o) \cos\left(\frac{\theta_{AB}}{2}\right) . \qquad (28)$$

These are the functions which result from the doppler mapping procedure with the approximations described above. They can be used in attempts to understand what information is contained in the doppler maps.

SECTION V

AMPLITUDE AND PHASE, MODULUS AND ARGUMENT

But it ought to be noted that although the forms of the received signals given in Equations (7) and (13) or the forms of the Fourier transforms given in Equations (24) and (27) are most convenient for certain types of analyses, they do not correspond directly to the forms that are actually determined by experiment. By this I mean that the measured signal is found in terms of its amplitude and phase at each instant of time, and the calculated doppler map is found in terms of its modulus and argument at each value of frequency shift. Therefore it may be useful in some future work to be able to express these measured quantities in terms of the variables which have appeared most suitable to the theoretical calculations. These expressions are exhibited below.

Consider first the received signals. It is well known that any complex number Z can be written in terms of amplitude A and phase Φ in the form

$$Z \equiv Ae^{j\Phi} , \tag{29}$$

where

$$A^2 \equiv ZZ^* \quad \text{and} \quad j \tan \Phi \equiv \frac{Z-Z^*}{Z+Z^*} . \tag{30}$$

Writing the received signal at site A in the form of Equation (7), and applying Equations (30), we find easily that

$$A^2(t) = \sum_{n=1}^{N} \sum_{m=1}^{N} H_n H_m \cos\left\{(\Psi_n - \Psi_m) - \frac{4\pi}{\lambda_o} \hat{R}_A \cdot [\vec{r}_n(t) - \vec{r}_m(t)]\right\} \tag{31a}$$

and

$$\tan \Phi(t) = \frac{\sum_{n=1}^{N} H_n \sin\left[\Psi_n - \frac{4\pi}{\lambda_o} \hat{R}_A(t) \cdot \vec{r}_n(t)\right]}{\sum_{n=1}^{N} H_n \cos\left[\Psi_n - \frac{4\pi}{\lambda_o} \hat{R}_A(t) \cdot \vec{r}_n(t)\right]}$$

The equivalent expressions for the case of reception at site B or site C are obvious, given Eq. (13).

In order to distinguish in terminology between the received signals and the calculated Fourier Transforms, we have adopted and shall consistantly use the following convention: we refer to the "amplitude" and "phase" of the signal, but we refer to the "modulus" and "argument" of the transform (or doppler map). In this terminology, we shall now find the modulus and argument of the transform function, using Equations (24) or (27). Let f_n be defined by either Equation (26) or Equation (28) as the case may be. Furthermore, let

$$F_n(f) \equiv TH_n \operatorname{sinc}\left[T(f - f_n)\right] \quad , \tag{32}$$

and let

$$\phi_n \equiv \Psi_n - 4\pi \frac{r_n}{\lambda_o} \hat{R}_A(t_o) \cdot \hat{r}_n(t_o) \tag{33a}$$

or

$$\phi_n \equiv \Psi_n - 4\pi \frac{r_n}{\lambda_o} \hat{R}_{AB}(t_o) \cdot \hat{r}_n(t_o) \cos\left(\frac{\theta_{AB}}{2}\right) \tag{33b}$$

as the case may be. Then Equations (24) or (27) can be written in the form:

$$\tilde{S}(f) \sim \sum_{n=1}^{N} F_n e^{j\phi_n} \quad . \tag{34}$$

We now write $\tilde{S}$ in the "mod and arg" form:

$$\tilde{S}(f) \sim M(f) e^{jA(f)} \quad , \tag{35}$$

and use the expressions analogous to Equations (30) to find that

$$M^2(f) = \sum_{n=1}^{N} \sum_{m=1}^{N} F_n(f) F_m(f) \cos(\phi_n - \phi_m) \, , \tag{36a}$$

and

$$\tan A(f) = \frac{\sum_{n=1}^{N} F_n(f) \sin \phi_n}{\sum_{n=1}^{N} F_n(f) \cos \phi_n} . \qquad (36b)$$

It is in connection with these formulae that an important point arises. With the approximations of Equations (15) and (17), we found that $F_n(f)$ was as given in Equation (32). The basic property of these functions F_n is that they are sharply peaked at $f = f_n$ and relatively small elsewhere; i. e., they are approximations to $\delta(f-f_n)$. It is reasonable to suspect that if different approximations were made, or if somehow the exact integrations could be performed, the forms of Equations (36) would remain unchanged, but the function F_n and ϕ_n might be somewhat altered. But if the approximation procedure is to mean anything at all, these functions cannot be changed very much. In particular we may assume that the more exact functions F_n are still sharply peaked at some values f_n which should not differ much from those values given in Equations (26) or (28), and that the more exact functions ϕ_n may now depend somehow on f but should not differ from Equations (33) to first order at least.

Now if $F_n(f)$ were very close to a true delta function (which would be the ideal situation), what should we expect to happen ? Equations (36) would then be effectively decoupled, in the sense that we would have

$$M(f) = \begin{cases} F_n(f_n) \text{ at } f = f_n \text{ for any } n \\ \\ \sim 0 \text{ at } f \neq f_n \text{ for any } n \end{cases}$$

$$A(f) = \begin{cases} \phi_n \text{ at } f = f_n \text{ for any } n \\ \\ \text{random at } f \neq f_n \text{ for any } n \end{cases}$$

Thereupon we could easily find the true values of f_n and ϕ_n (mod 2π) and be well on the way towards solving for the locations and motions of all the scatterers. But if $F_n(f)$ is not very close to a perfect delta function but rather has significant sidelobes (as for example in the form Equation (32), since the first sidelobes of the sinc function are down by only about 6 db), then the different terms of Equations (36) become seriously cross-coupled. This intermodulation has three deleterious effects, all of which can easily be observed in the case of the sinc function:

1. Spurious peaks may appear in the modulus function at values of f not corresponding to any true scatterer.

2. The values of f at which genuine peaks appear in the modulus function are somewhat displaced from the correct values f_n.

3. The values of the argument corresponding to peaks in the modulus function are somewhat displaced from the correct values ϕ_n.

These problems can, if sufficiently severe, make correct interpretation of the data rather difficult. Therefore it is important to try to insure that the functions $F_n(f)$ are reasonably good approximations to delta functions.

Naturally, we can't change the data as the target presents them to us. But it may be possible to take steps during the Fourier integration procedure to ensure that the functions F_n have high, narrow peaks and low sidelobe levels. Amplitude weighting, for example, can considerably reduce the sidelobes, but only at the cost of some broadening of the peaks. Increasing the integration time T with the help of previously estimated body motion constraints might go a long way toward alleviating this problem, if it can be done.

SECTION VI

SOME CONSIDERATIONS ON USING THE DATA

If we can ignore the complications of intermodulation described above, and if we may assume the approximations to be reasonable ones, then the Fourier transform function (doppler map) contains two sorts of information about the target. The frequency shift, f, corresponding to each peak in the modulus function is related via Eq. (26) or (28) to the angular velocity vector of the target and to the "cross range" component of the location of one of the scattering centers relative to the target center. And the value of the argument corresponding to each such peak in the modulus contains information concerning the "down range" component of scattering center location (unfortunately corrupted by the unknown intrinsic phase shift Ψ_n). The argument information is quite precise but ambiguous; the modulus information is less precise but unambiguous. Reference 1 described how the argument information could be used, but ignored the modulus information. It seems very reasonable to think that the best way to handle the data is to use both types of information together to refine our knowledge both of the locations of the scattering centers and of the body motion of the target. A more detailed scheme for doing this will be presented in a subsequent paper, together with considerations of errors and uncertainties in the method and of their possible effects.

REFERENCE

1 N. M. Tomljanovich, H. S. Ostrowsky, J. F. A. Ormsby, "Narrowband Interferometer Imaging," ESD-TR-68-274, The MITRE Corporation, Bedford, Mass., Nov. 1968.

14 KEY WORDS	LINK A		LINK B		LINK C	
	ROLE	WT	ROLE	WT	ROLE	WT
NARROWBAND INTERFEROMETRY						
ELECTROMAGNETIC SCATTERING						